J|A|C|S
ARTICLES
Published on Web 04/01/2006

Inverse Miniemulsion ATRP: A New Method for Synthesis and Functionalization of Well-Defined Water-Soluble/ Cross-Linked Polymeric Particles

Jung Kwon Oh, Chuanbing Tang, Haifeng Gao, Nicolay V. Tsarevsky, and Krzysztof Matyjaszewski*

Contribution from the Center for Macromolecular Engineering, Department of Chemistry, Carnegie Mellon University, 4400 Fifth Avenue, Pittsburgh, Pennsylvania 15213

Received February 1, 2006; E-mail: km3b@andrew.cmu.edu

Abstract: A new methodology for the synthesis and functionalization of nanometer-sized colloidal particles consisting of well-defined, water-soluble, functional polymers with narrow molecular weight distribution ($M_w/M_n < 1.3$) was developed, utilizing atom transfer radical polymerization (ATRP) of water-soluble monomers in an inverse miniemulsion. The optional introduction of a disulfide-functionalized cross-linker allowed for the synthesis of cross-linked (bio)degradable nanogels. Dynamic light scattering (DLS) and atomic force microscopy (AFM) measurements indicated that these particles possessed excellent colloidal stability. ATRP in inverse miniemulsion led to materials with several desirable features. The colloidal particles preserved a high degree of halogen chain-end functionality, which enabled further functionalization. Cross-linked nanogels with a uniformly cross-linked network were prepared. They were degraded to individual polymeric chains with relatively narrow molecular weight distribution ($M_w/M_n < 1.5$) in a reducing environment. Higher colloidal stability, higher swelling ratios, and better controlled degradability indicated that the nanogels prepared by ATRP were superior to their corresponding counterparts prepared by conventional free radical polymerization (RP) in inverse miniemulsion.

Introduction

Controlled/living radical polymerization (CRP) provides a versatile route for synthesis of (co)polymers with narrow molecular weight distribution, designed architectures, and useful end functionalites.[1−3] Various methods for CRP include atom transfer radical polymerization (ATRP),[4−7] stable free radical polymerization (SFRP),[8,9] degenerative transfer polymerization (DT) with alkyl iodides,[10,11] reversible addition−fragmentation transfer polymerization (RAFT),[12−14] and cobalt-mediated radical polymerization (CMRP).[15−17] CRP reactions have been examined in heterogeneous aqueous dispersions primarily due to environmental benefits, better process control, and the feasibility of commercial production of latex particles. However, from a research perspective, conducting CRP in biphasic media is more complicated and challenging than in homogeneous bulk and solution conditions. Several reviews[18−21] and papers concerning CRP in aqueous dispersion were recently published, including ATRP,[22−26] SFRP,[27−30] and RAFT.[31−33] Most efforts have been directed at CRP of hydrophobic monomers using

(1) Matyjaszewski, K., Davis, T. P., Eds. *Handbook of Radical Polymerization*; John Wiley & Sons Inc.: New York, 2002.
(2) Davis, K. A.; Matyjaszewski, K. *Adv. Polym. Sci.* **2002**, *159*, 2−166.
(3) Coessens, V.; Pintauer, T.; Matyjaszewski, K. *Prog. Polym. Sci.* **2001**, *26*, 337−377.
(4) Wang, J.-S.; Matyjaszewski, K. *J. Am. Chem. Soc.* **1995**, *117*, 5614−5615.
(5) Patten, T. E.; Xia, J.; Abernathy, T.; Matyjaszewski, K. *Science* **1996**, *272*, 866−868.
(6) Kamigaito, M.; Ando, T.; Sawamoto, M. *Chem. Rev.* **2001**, *101*, 3689−3745.
(7) Matyjaszewski, K.; Xia, J. *Chem. Rev.* **2001**, *101*, 2921−2990.
(8) Georges, M. K.; Veregin, R. P. N.; Kazmaier, P. M.; Hamer, G. K. *Macromolecules* **1993**, *26*, 2987−2988.
(9) Hawker, C. J.; Bosman, A. W.; Harth, E. *Chem. Rev.* **2001**, *101*, 3661−3688.
(10) Gaynor, S. G.; Wang, J.-S.; Matyjaszewski, K. *Macromolecules* **1995**, *28*, 8051−8056.
(11) Iovu, M. C.; Matyjaszewski, K. *Macromolecules* **2003**, *36*, 9346−9354.
(12) Chiefari, J.; Chong, Y. K.; Ercole, F.; Krstina, J.; Jeffery, J.; Le, T. P. T.; Mayadunne, R. T. A.; Meijs, G. F.; Moad, C. L.; Moad, G.; Rizzardo, E.; Thang, S. H. *Macromolecules* **1998**, *31*, 5559−5562.
(13) Chiefari, J.; Rizzardo, E. In *Handbook of Radical Polymerization*; Davis, T. P., Ed.; John Wiley & Sons Inc.: New York, 2002; p 629.
(14) Perrier, S.; Takolpuckdee, P. *J. Polym. Sci., Part A: Polym. Chem.* **2005**, *43*, 5347−5393.
(15) Wayland, B. B.; Poszmik, G.; Mukerjee, S. L.; Fryd, M., *J. Am. Chem. Soc.* **1994**, *116*, 7943−7944.
(16) Debuigne, A.; Caille, J.-R.; Jerome, R. *Angew. Chem., Int. Ed.* **2005**, *44*, 1101−1104.
(17) Kaneyoshi, H.; Matyjaszewski, K. *Macromolecules* **2005**, *38*, 8163−8169.
(18) Qiu, J.; Charleux, B.; Matyjaszewski, K. *Prog. Polym. Sci.* **2001**, *26*, 2083−2134.
(19) Cunningham, M. F. *Prog. Polym. Sci.* **2002**, *27*, 1039−1067.
(20) Asua, J. M. *Prog. Polym. Sci.* **2002**, *27*, 1283−1346.
(21) Schork, F. J.; Luo, Y.; Smulders, W.; Russum, J. P.; Butte, A.; Fontenot, K. *Adv. Polym. Sci.* **2005**, *175*, 129−255.
(22) Li, M.; Matyjaszewski, K. *Macromolecules* **2003**, *36*, 6028−6035.
(23) Li, M.; Jahed, N. M.; Min, K.; Matyjaszewski, K. *Macromolecules* **2004**, *37*, 2434−2441.
(24) Li, M.; Min, K.; Matyjaszewski, K. *Macromolecules* **2004**, *37*, 2106−2112.
(25) Min, K.; Matyjaszewski, K. *Macromolecules* **2005**, *38*, 8131−8134.
(26) Min, K.; Gao, H.; Matyjaszewski, K. *J. Am. Chem. Soc.* **2005**, *127*, 3825−3830.
(27) Szkurhan, A. R.; Georges, M. K. *Macromolecules* **2004**, *37*, 4776−4782.
(28) Cunningham, M.; Lin, M.; Buragina, C.; Milton, S.; Ng, D.; Hsu, C. C.; Keoshkerian, B. *Polymer* **2005**, *46*, 1025−1032.
(29) Nicolas, J.; Charleux, B.; Guerret, O.; Magnet, S. *Macromolecules* **2005**, *38*, 9963−9973.
(30) Nicolas, J.; Charleux, B.; Guerret, O.; Magnet, S. *Angew. Chem., Int. Ed.* **2004**, *43*, 6186−6189.
(31) Ferguson, C. J.; Hughes, R. J.; Nguyen, D.; Pham, B. T. T.; Gilbert, R. G.; Serelis, A. K.; Such, C. H.; Hawkett, B. S. *Macromolecules* **2005**, *38*, 2191−2204.

10.1021/ja060586a CCC: $33.50

conventional emulsion, microemulsion, miniemulsion, and suspension polymerization and have resulted in the successful synthesis of stable latex particles consisting of well-defined, hydrophobic polymers. However, to the best of our knowledge, a CRP of water-soluble or hydrophilic monomers in inverse miniemulsion has not yet been reported. Herein, we report the first CRP of water-soluble monomers in an inverse miniemulsion, a process that allows for the controlled synthesis of nanometer-sized colloidal particles of water-soluble polymers.

Inverse miniemulsion polymerization is a heterogeneous water-in-oil (W/O) polymerization process that can be applied to the synthesis of hydrophilic and water-soluble polymeric particles. This process involves aqueous droplets (including water-soluble monomers), stably dispersed with the aid of oil-soluble surfactants in a continuous organic media by sonification.[34] Polymerization occurs within the aqueous droplets producing stable colloidal particles upon the addition of radical initiators. Recent reports have demonstrated the synthesis of hydrophilic or water-soluble particles of poly(2-hydroxyethyl methacrylate) (PHEMA), poly(acrylamide) (PAAm) and poly(acrylic acid) (PAA),[35−37] and temperature-sensitive hollow microspheres of poly(*N*-isopropylacrylamide) (PNIPAM).[38] However, due to the use of uncontrolled free-radical polymerization processes (RP), all of these examples resulted in the preparation of polymers with broad molecular weight distribution (i.e., $M_w/M_n > 2.0$) and without chain-end functionality.

Precipitation polymerization is an alternative method that has been utilized to prepare cross-linked colloidal particles in aqueous media.[39,40] The resulting hydrogel particles consist of water-soluble and hydrophilic homopolymers and copolymers of poly(*N*-alkyl(meth)acrylamide), typically PNIPAM, and PAA.[41−43] However, a significant amount of cross-linking agent has to be used to isolate the particles from the reaction media.

We have developed a new methodology for synthesizing and functionalizing nanometer-sized colloidal particles consisting of water-soluble functional polymers with narrow molecular weight distribution. Our approach involves the utilization of a new initiation process for ATRP-named activators generated by electron transfer (i.e., AGET ATRP)[26,44] for the polymerization of water-soluble monomers in an inverse miniemulsion. The additional introduction of a functional cross-linker, such as a disulfide,[45,46] allows for the synthesis of cross-linked (bio)-degradable nanoparticles (well-defined nanogels). Application of this methodology results in the preparation of materials with the following features: (1) The colloidal particles preserve a high degree of halide end functionality. This halide functionality enables further chain extension and formation of block copolymers and/or functionalization with biorelated molecules, e.g. through highly efficient "Click Chemistry"[47−49] resulting in the preparation of polymer−biomolecule conjugates.[50,51] (2) Due to the utilization of a controlled radical polymerization (CRP) process, namely ATRP, nanogels with a uniformly cross-linked network can be prepared.[52] (3) In a reducing environment the cross-linked nanogels can degrade to individual polymeric chains with relatively narrow molecular weight distribution ($M_w/M_n < 1.5$). Disulfide groups have been reported to degrade into the corresponding thiols in the presence of tributyl phosphine (Bu_3P)[45] or dithiothreitol.[46,53]

These unique properties suggest that the well-defined functional nanogels hold great potential as carriers for controlled drug delivery scaffolds to target specific cells. Drugs can be loaded into the nanogels. In a reducing environment the nanogels will degrade to individual polymeric chains with a molecular weight below the renal threshold, thus controllably releasing the encapsulated drugs over a desired period of time.[54,55]

Here we describe the first step toward meeting these long-term research goals by demonstrating a versatile approach to functional nanogels utilizing an inverse miniemulsion ATRP. Our approach allows for the synthesis of nanoparticles of well-defined, water-soluble polymers and, in the presence of an added disulfide-functionalized cross-linker, nanogels with a uniform cross-linked network. The results of morphology, swelling behavior, and degradation studies indicate that the nanogels prepared by ATRP possess better colloidal stability, a larger swelling ratio, and better degradation behavior, rendering them superior to their corresponding counterparts prepared by conventional free radical polymerization (RP) in inverse miniemulsion. The preservation of bromine functionality in the ATRP-nanogels was demonstrated by successful chain extension of the active terminal functionality present throughout the nanogels by the ATRP of styrene, resulting in the formation of nanogel-*ce*-polystyrene (PS) copolymers (where *-ce-* is an abbreviation for "Chain Extended" to indicate that the chain extension is throughout the nanoparticle, not only from the particle surface) (Scheme 1).

Results and Discussion

The synthesis and functionalization of nanometer-sized colloidal particles consisting of well-defined, water-soluble polymers via ATRP was accomplished by inverse miniemulsion. Oligo(ethylene glycol) monomethyl ether methacrylate (OEOMA) with different molecular weights, OEOMA300 ($M = 300$ g/mol, pendent EO units DP ≈ 7) and OEOMA1100 ($M = 1100$ g/mol, pendent EO units DP ≈ 23), was chosen as the water-

(32) Biasutti, J. D.; Davis, T. P.; Lucien, F. P.; Heuts, J. P. A. *J. Polym. Sci., Part A: Polym. Chem.* **2005**, *43*, 2001−2012.
(33) Bussels, R.; Bergman-Goettgens, C.; Meuldijk, J.; Koning, C. *Polymer* **2005**, *46*, 8546−8554.
(34) Antonietti, M.; Landfester, K. *Prog. Polym. Sci.* **2002**, *27*, 689−757.
(35) Landfester, K.; Willert, M.; Antonietti, M. *Macromolecules* **2000**, *33*, 2370−2376.
(36) Willert, M.; Landfester, K. *Macromol. Chem. Phys.* **2002**, *203*, 825−836.
(37) Wormuth, K. *J. Colloid Interface Sci.* **2001**, *241*, 366−377.
(38) Sun, Q.; Deng, Y. *J. Am. Chem. Soc.* **2005**, *127*, 8274−8275.
(39) Pelton, R. H.; Chibante, P. *Colloid Surf.* **1986**, *20*, 247−256.
(40) Wu, X.; Pelton, R. H.; Hamielec, A. E.; Woods, D. R.; McPhee, W. *Colloid Polym. Sci.* **1994**, *272*, 467−477.
(41) Stayton, P. S.; Shimoboji, T.; Long, C.; Chilkoti, A.; Chen, G.; Harris, J. M.; Hoffman, A. S. *Nature* **1995**, *378*, 472−474.
(42) Zhang, J.; Xu, S.; Kumacheva, E. *J. Am. Chem. Soc.* **2004**, *126*, 7908−7914.
(43) Kim, J.; Nayak, S.; Lyon, L. A. *J. Am. Chem. Soc.* **2005**, *127*, 9588−9592.
(44) Jakubowski, W.; Matyjaszewski, K. *Macromolecules* **2005**, *38*, 4139−4146.
(45) Tsarevsky, N. V.; Matyjaszewski, K. *Macromolecules* **2005**, *38*, 3087−3092.
(46) Li, Y.; Armes, S. P. *Macromolecules* **2005**, *38*, 8155−8162.
(47) Tsarevsky, N. V.; Sumerlin, B. S.; Matyjaszewski, K. *Macromolecules* **2005**, *38*, 3558−3561.
(48) Opsteen, J. A.; van Hest, J. C. M. *Chem. Commun.* **2005**, 57−59.
(49) Lutz, J.-F.; Boerner, H. G.; Weichenhan, K. *Macromol. Rapid Commun.* **2005**, *26*, 514−518.
(50) Devaraj, N. K.; Miller, G. P.; Ebina, W.; Kakaradov, B.; Collman, J. P.; Kool, E. T.; Chidsey, C. E. D. *J. Am. Chem. Soc.* **2005**, *127*, 8600−8601.
(51) Hawker, C. J.; Wooley, K. L. *Science* **2005**, *309*, 1200−1205.
(52) Isaure, F.; Cormack, P. A. G.; Graham, S.; Sherrington, D. C.; Armes, S. P.; Buetuen, V. *Chem. Commun.* **2004**, 1138−1139.
(53) Tsarevsky, N. V.; Matyjaszewski, K. *Macromolecules* **2002**, *35*, 9009−9014.
(54) Huang, X.; Lowe, T. L. *Biomacromolecules* **2005**, *6*, 2131−2139.
(55) Eichenbaum, K. D.; Thomas, A. A.; Eichenbaum, G. M.; Gibney, B. R.; Needham, D.; Kiser, P. F. *Macromolecules* **2005**, *38*, 10757−10762.

Scheme 1. Illustration of a New Approach for Synthesis and Functionalization of Nanometer-Sized Colloidal Particles of Well-Controlled Water-Soluble Polymers with Narrow Molecular Weight Distribution

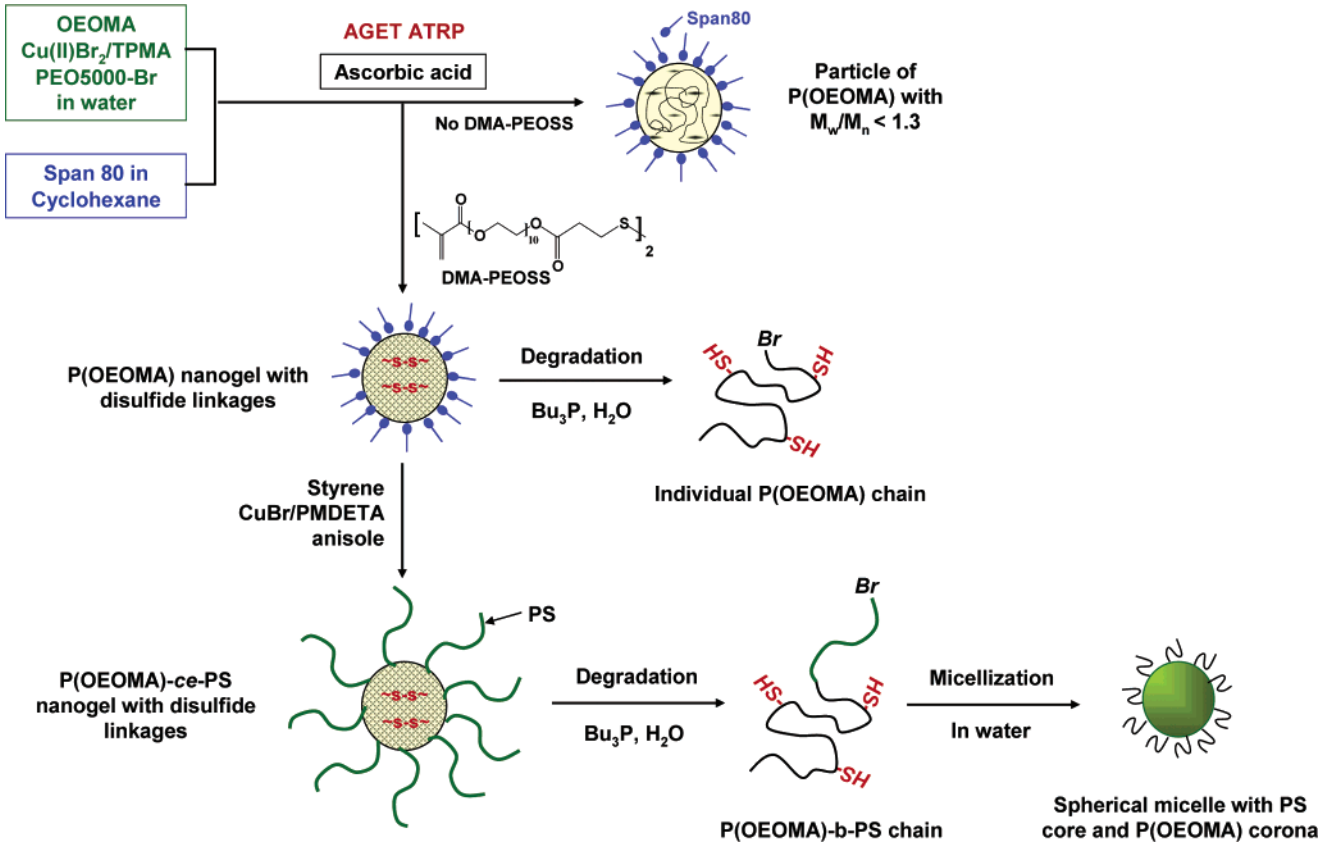

soluble monomer to demonstrate the utility of the system. Poly(ethylene glycol) (PEO) is biocompatible, has low toxicity, and prevents nonspecific protein adsorption and cell adhesion.[56] The correct selection of a suitable surfactant is crucial to ensure colloidal stability of inverse miniemulsion. Commercially available Span 80 (sorbitan monooleate, HLB = 4.3) was previously used for the synthesis of stable latex particles of PAAm using RP in inverse miniemulsion.[35] Similarly, in our turbidity experiments, Span 80 formed a stable inverse miniemulsion of OEOMA with water in cyclohexane, allowing for the synthesis of stable P(OEOMA) particles. Other oil-soluble surfactants, including poly(propylene glycol)-*b*-poly(ethylene glycol)-*b*-poly(propylene glycol) (PPO-*b*-PEO-*b*-PPO, 10% PEO, M = 3300 g/mol, HLB = 2) and Span 85 (sorbitan trioleate, HLB = 1.8) did not form stable inverse miniemulsion systems. Water was used as a solvent to form an aqueous phase as well as a lipophobe to build up an osmotic pressure in inverse miniemulsion droplets.

In addition to colloidal stability, several other requirements should be met to conduct a successful inverse miniemulsion ATRP. Since polymerization occurs in the aqueous monomer droplets dispersed in an organic media, all ATRP ingredients including catalyst, ligand, and initiator must be soluble in water. This requires preferential partitioning of the copper complex and initiator into the aqueous phase. A water-soluble, PEO-functionalized bromoisobutyrate (PEO5000-Br) was synthesized and used as the initiator for the preparation of PEO-*block*-P(OEOMA) copolymers. As an additional requirement, the ATRP activator and deactivator must be stable in water. For example, dissociation of the Br−Cu(II) bond in water could result in a reduction of the rate of deactivation, leading to a loss of control.[57] These problems were overcome by using tris-[(2-pyridyl)methyl]amine (TPMA) as the ligand forming a complex with $CuBr_2$ as the catalyst precursor. TPMA is known to provide an active water-soluble complex, which has low tendency for disproportionation.[58] The AGET ATRP process involves the use of an oxidatively stable Cu(II) precursor that can generate the active Cu(I) catalyst by reaction with nonradical-forming reducing agents. Consequently, the concentration of the Cu(II) complex, the deactivator, can be controlled throughout the reaction, leading to improved control over initiation and propagation.[26,44] Water-soluble ascorbic acid was used as the reducing agent.

Synthesis of Uncross-Linked Colloidal Particles of Water-Soluble Well-Controlled P(OEOMA) by AGET ATRP in Inverse Miniemulsion. Table 1 presents the results of a series of experiments conducted where the amount of Cu(II) complex initially added to the reaction was varied in an inverse miniemulsion AGET ATRP of OEOMA1100 at 30 °C. The experimental results show that all polymerizations produced nanometer-sized particles with excellent colloidal stability. As an example, Figure 1 illustrates a size distribution diagram plot for water-soluble P(OEOMA1100) colloidal particles stably dispersed in cyclohexane. DLS measurements show the size of the particles to be around 188−207 nm in diameter with narrow size distribution (CV = 0.03−0.09). Polymerization proceeded up to 90% conversion for all three initiator/catalyst ratios.

(56) Brannon-Peppas, L. *J. Controlled Release* **2000**, *66*, 321.

(57) Tsarevsky, N. V.; Pintauer, T.; Matyjaszewski, K. *Macromolecules* **2004**, *37*, 9768−9778.

(58) Tsarevsky, N. V.; Matyjaszewski, K. *ACS Symp. Ser.* **2006**, 937. In press.

Table 1. Preparation of Nanometer-Sized Colloidal Particles of Well-Controlled P(OEOMA1100) by AGET ATRP of OEOMA1100 in Inverse Miniemulsion at 30 °C with Various Ratios of Initiator to Cu(II) Complex[a]

$[OEOMA1100]_0/[PEO5000\text{-}Br]_0/[Cu_2Br/TPMA]_0$	time/min	conv.	$M_{n,theo}$[b]	$M_{n,GPC}$	M_w/M_n	D_{av}[c] (nm)	CV[c]
70/1/1	35	0.88	73 000	65 800	1.33	188	0.09
70/1/0.5	50	0.88	73 000	67 200	1.29	207	0.07
70/1/0.3	90	0.93	77 000	69 100	1.46	205	0.03

[a] Conditions: OEOMA1100/water = 1/1 v/v; solids content = 10 wt %; $[CuBr_2/TPMA]_0/[\text{ascorbic acid}]_0 = 1/0.7$. [b] $M_{n,theo}$ = MW (PEO5000−Br) + MW(OEOMA1100) x ($[OEOMA1100]_0/[PEO5000\text{−}Br]_0$) x conversion. [c] D_{av} is average diameter, and CV (coefficient of variation) is size distribution index, which are defined as follows, $D_{av} = \sum_{i=1}^{n} D_i/n$; $S = [\sum_{i=1}^{n}(D_i - D_{av})^2(n-1)]^{1/2}$; $CV = S/D_{av}$, where D_i is the diameter of the particle *i*, *n* is the total number counted, and *S* is the size standard deviation.

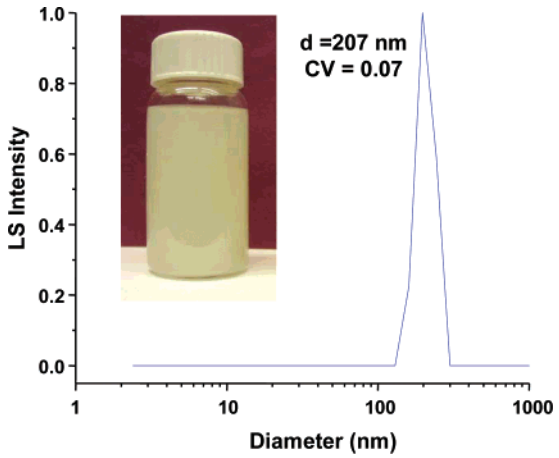

Figure 1. Size distribution diagram of water-soluble P(OEOMA1100) colloidal particles prepared by AGET ATRP in inverse miniemulsion at 30 °C. (Inset) Digital image of the dispersion of particles in cyclohexane. Conditions: $[OEOMA1100]_0/[PEO5000\text{-}Br]_0/[CuBr_2/TPMA]_0/[\text{ascorbic acid}]_0 = 70/1/0.5/0.35$; OEOMA1100/water = 1/1 v/v; solids content = 10 wt %.

However, the best results were obtained for the ratio of initiator to Cu(II) complex of around 1/0.5. As shown in Figure S1, polymerization was first order, indicating a constant concentration of active centers during the reaction. The polymerization was well controlled. Molecular weight increased monotonically with conversion, and polydispersity remained low, $M_w/M_n < 1.3$ up to 90% conversion.

Several AGET ATRP reactions were also conducted with OEOMA300 in an inverse miniemulsion with cyclohexane as the suspending medium at 30 °C under the similar experimental conditions. As shown in Figure 2, the polymerization was well controlled, and molecular weight increased with conversion, producing P(OEOMA300) with narrow molecular distribution (M_w/M_n <1.3) in the resulting stable, colloidal particles. The DLS measurements show that the average particle size was in the range of 120−150 nm with narrow size distribution (CV = 0.03−0.06) (Figure S2). The particle size of P(OEOMA300) was smaller than that of P(OEOMA1100), d = 200 nm on average. This difference can be attributed to the more hydrophobic character of OEOMA300. This will result in the partitioning of some OEOMA300 into the organic phase as well as the tending to stay on the particle surface to reduce interfacial tension and therefore particle size, compared to OEOMA1100.

The above results confirm that this new strategy involving ATRP and inverse miniemulsion polymerization techniques

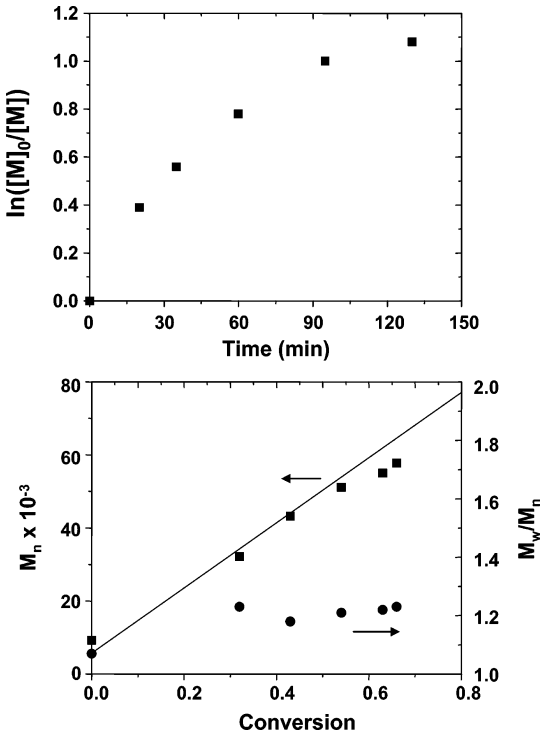

Figure 2. Kinetic plot (top) and evolution of molecular weight and molecular weight distribution with conversion (bottom) for AGET ATRP of OEOMA300 in inverse miniemulsion of cyclohexane at 30 °C. Conditions: $[OEOMA300]_0/[PEO5000\text{-}Br]_0/[CuBr_2/TPMA]_0/[\text{ascorbic acid}]_0 = 300/1/0.5/0.35$; OEOMA300/water = 1/1 v/v; solids content = 10 wt %; The straight line is the theoretically predicted molecular weight over conversion. Molecular weights of P(OEOMA300) were calibrated with PMMA standards.

Scheme 2. Preparation of a Disulfide-Functionalized Dimethacrylate Crosslinker (**1**)[a]

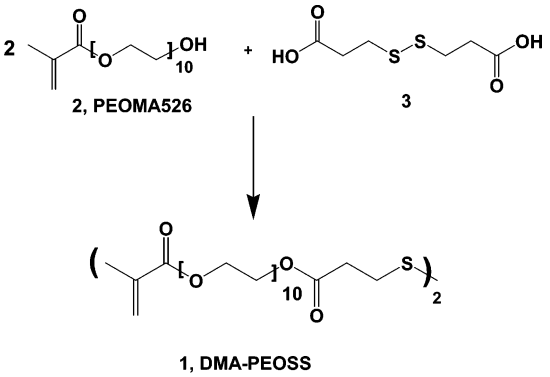

[a] Conditions: dicyclohexylcarbodiimide (DCC), 4-(dimethylamino)pyridine (DMAP), THF, and CH_2Cl_2 at 0°C.

allows for the synthesis of well-defined, nanometer-sized colloidal particles consisting of water-soluble P(OEOMA) with narrow molecular weight distribution (M_W/M_n < 1.3).

Comparison of P(OEOMA300) Nanogels Formed in Inverse Miniemulsion in the Presence of Dimethacrylate Cross-Linker by AGET ATRP with Nanogels Prepared by RP. The optimized procedure was applied to the synthesis of (bio)degradable, cross-linked P(OEOMA300) particles. A cross-linking agent based on a disulfide-functionalized dimethacrylate (DMA-PEOSS) was synthesized as shown in Scheme 2 and introduced into an inverse miniemulsion ATRP. The synthesis of P(OEOMA300) nanogels was accomplished by adding 1.5 mol % of DMA-PEOSS to an inverse miniemulsion AGET

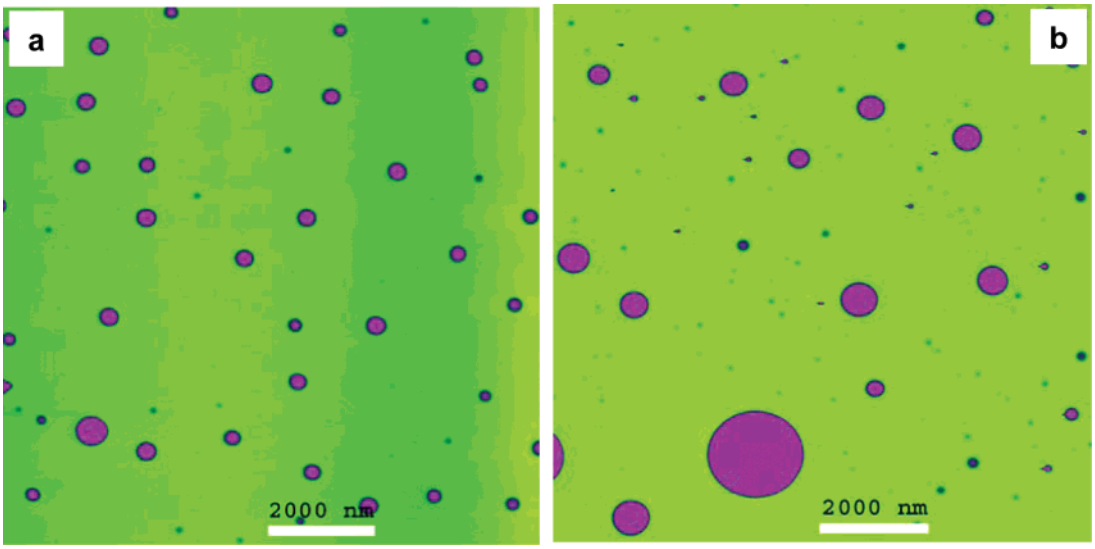

Figure 3. AFM height images of uncross-linked (a) and cross-linked (b) colloidal particles of P(OEOMA300) prepared in the absence and presence of 1.5 mol % dimethacrylate cross-linker (**1**) by inverse miniemulsion ATRP at 30 °C. Each image frame is 10 μm × 10 μm.

Table 2. Characterization Data for P(OEOMA300) Colloidal Particles Prepared by Inverse Miniemulsion AGET ATRP at 30 °C

	DLS		AFM[a]			
	D_{av} (nm)	CV	$H_{n,av}$ (nm)	$H_{w,av}/H_{n,av}$	$D_{n,av}$ (nm)	$D_{av,w}/D_{av,n}$
uncross-linked	145	0.03	18 ± 6	1.11	310 ± 88	1.08
cross-linked	260	0.15	55 ± 23	1.17	425 ± 171	1.15

[a] $H_{n,av}$ and $D_{n,av}$ are the number average height and diameter, and $H_{w,av}$ and $D_{w,av}$ are the weight average height and diameter, respectively.

Table 3. Comparison of Properties of Degradable Nanogels Prepared by Inverse Miniemulsion ATRP with RP

	swelling ratio[a] in:				
	THF	toluene	water	M_n,[b] kg/mol	M_w/M_n[b]
ATRP-nanogels	21.3	19.6	28.5	74	1.5
RP-nanogels	13.1	13.1	16.2	not degraded	

[a] Expressed as grams of solvent absorbed by gram of dry gel. [b] GPC analysis of the products of reductive degeneration with Bu_3P in THF for 3 days.

ATRP of OEOMA300 at ambient temperature (30 °C). The resulting particles did not dissolve in any solvent, including THF and water. This indicates that the particles were cross-linked during the polymerization. A small amount of larger particles (less than 0.5 wt % of total solids) was observed, suggesting the formation of aggregates during polymerization in the presence of the cross-linker. DLS measurements indicate that the size of the cross-linked particles dispersed in cyclohexane was 260 nm in diameter with a relatively broad size distribution (CV = 0.15). In general, the size of cross-linked particles was larger than that of uncross-linked particles dispersed in cyclohexane.

The morphology of both uncross-linked and cross-linked colloidal particles was analyzed by tapping mode AFM. Figure 3 shows the AFM images of uncross-linked (a) and cross-linked (b) colloidal P(OEOMA300) particles on mica surface. The particle size distribution was narrow for uncross-linked particles (a) but broader for cross-linked particles (b), as expected from DLS measurements. The average diameter of the uncross-linked particles, (without the correction of tip contribution) determined by AFM analysis was 310 nm, i.e., ~2 times larger than that determined by DLS (Table 2). The difference is due to flattening of the particles on the mica surface during the casting process, as confirmed by the smaller height (18 nm). Interestingly, the difference decreased when the particles were cross-linked; the ratio of the sizes determined by AFM (425 nm) to that by DLS (260 nm) was 1.6 times. This is because cross-linked particles spread out on the mica surface to a lesser degree, as confirmed by their relatively larger height (55 nm compared to 18 nm).

The experimental details, including kinetic data, for both uncross-linked and cross-linked P(OEOMA300) particles prepared using an inverse miniemulsion RP in the absence and presence of 1.5 mol % DMA-PEOSS are provided in Supporting Information. 2,2-Azobis(4-methoxy-2,4-dimethylvaleronitrile) (V-70, Wako Chemie) was used to initiate an inverse miniemulsion polymerization of OEOMA300 at the relatively low temperature of 40 °C. In the absence of DMA-PEOSS, the polymerization proceeded to 89% conversion within 4 h and produced colloidal particles of P(OEOMA300) with M_n = 61 400 g/mol and M_w/M_n = 2.2 (Figure S3). In the presence of 1.5 mol % cross-linker, cross-linked particles were produced. However, both uncross-linked and cross-linked particles prepared by RP were precipitated out of the dispersion within 1 day.

Table 3 compares the swelling ratios and degradation behavior of nanogels prepared by ATRP (i.e., ATRP-nanogels) with nanogels prepared by RP (i.e., RP-nanogels). Both gels were prepared in the presence of 1.5 mol % DMA-PEOSS. The purified, dried nanogels were swollen in different solvents including THF, toluene, and water. Swelling ratios of nanogels were determined by the weight ratio of wet gels to dried gels. For ATRP-nanogels, the swelling ratios ranged from ~20 in organic solvents (THF and toluene) to ~28 in water. These values were 1.6−1.8 times larger than those for RP-nanogels in all solvents examined. This difference could be ascribed to the cross-links being more evenly distributed in the ATRP nanogels.

The reductive degradation of the nanogels to the corresponding thiol-containing P(OEOMA300) fragments was conducted in the presence of Bu_3P in THF over 3 days. In the case of the ATRP-nanogels, the degraded polymers had M_n = 74 000 g/mol

and $M_w/M_n = 1.5$. These values are somewhat larger than $M_n = 55\,000$ g/mol and $M_w/M_n = 1.2$ for uncross-linked P(OEOMA300). This difference may be due to either incomplete degradation of disulfide linkages or formation of irreversible cross-links by the trace amount of PEO-dimethacrylate contained in PEOMA526 (shoulder on a GPC trace in Figure S5a).[59] For RP-nanogels, the mixtures of nanogels and Bu_3P in THF were stirred for over a week. However, they could not be filtered through a 0.2-μm PFFT filter, indicating that insignificant degradation of the RP-nanogels occurred.

These results clearly demonstrated that inverse miniemulsion ATRP in the presence of a cross-linker resulted in the formation of nanogels with a uniform network structure that could degrade into the corresponding linear polymers in a reducing environment. The ATRP-nanogels had larger swelling ratios than RP-nanogels in various solvents. They could be redispersed in water without the aid of additional surfactants to form stable hydrogels with a large swelling ratio of 28. Moreover, the degraded P(OEOMA300) is biocompatible, has low toxicity, and prevents nonspecific adsorption to cells. These unique properties make the nanometer-sized hydrogels promising candidates for drug delivery scaffolds.

ATRP Chain Extension with Polystyrene from ATRP-P(OEOMA300) Nanogels. Polymers prepared by ATRP preserve a halogen end functionality. Therefore ATRP-nanogels are capable of further functionalization. The preservation of bromine functionality within the ATRP-nanogels was demonstrated by an ATRP chain extension with polystyrene from the purified ATRP-nanogel macroinitiators, followed by degradation of nanogel-*ce*-PS copolymers. As shown in Figure S4, the first-order kinetic plot for the chain extension shows that conversion rapidly reached 20% after 2 h, and then gradually increased to 30% over the remaining 19 h. This change in rate of conversion with time may be attributed to nonuniform distribution of bromine functional groups throughout the core and on the surface of the nanoparticles. The molecular weight distribution data support this assumption.

Aliquots of the copolymer samples taken at 7 h and at the end of reaction (21 h) were subjected to degradation in the presence of Bu_3P in THF and then were injected into GPC without purification. Figure S5 shows the evolution of GPC traces of the degraded P(OEOMA300) homopolymer (a) and P(OEOMA300)-*block*-PS copolymers taken at time intervals of 7 and 21 h (b and c). Molecular weight increased with conversion, indicating the successful growth of PS chains from active ATRP initiating sites within the P(OEOMA300) nanogels. However, molecular weight distribution of degraded P(OEOMA300)-*block*-PS copolymers was broader ($M_w/M_n = 1.9-2.2$), compared with the value ($M_w/M_n = 1.5$) for degraded P(OEOMA300) homopolymer. This broadening of the M_w/M_n values for the block copolymers may be caused by the more difficult access of catalysts into the core, compared to the surface of particles. An interesting observation is that the GPC traces of resulting block copolymers had monomodal distributions.[60] For example, at 30% conversion, the weight ratio of PS to P(OEOMA300) gel can be calculated as 54/46 wt/wt. If a significant amount of free P(OEOMA300) chains existed in the reaction mixture, the GPC traces should be bimodal. The GPC results indicate that in gel particles a large majority of P(OEOMA) chains were chain extended with polystyrene.

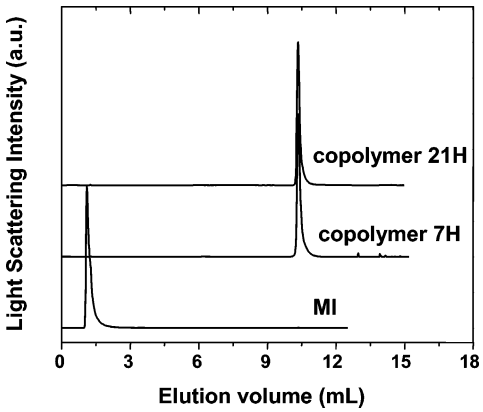

Figure 4. HPLC chromatograms of P(OEOMA300) macroinitiator (MI) and P(OEOMA300)-*block*-PS taken at different time intervals of 7 and 21 h. All polymers degraded in the presence of Bu_3P at room temperature for 3 days and were purified by precipitation from hexane.

HPLC Analysis and Micellization of Degraded P(OEOMA300)-*block*-PS Copolymers. Further investigation was attempted using HPLC chromatography, in which polymers were eluted according to their compositions. This method allowed for the separation of P(OEOMA300)-*block*-PS copolymers from P(OEOMA300) homopolymers. Aliquots of the above samples taken at 7 and 21 h were purified by precipitation from hexane. Since hexane is a poor solvent for both polymers consisting of PS and P(OEOMA300) but a good solvent for styrene monomer, both P(OEOMA300)-*block*-PS and P(OEOMA300) can be precipitated. Figure 4 clearly indicates that there is not a significant amount of P(OEOMA300) macroinitiators left in the reaction mixture. In other words, most P(OEOMA300) chains were functionalized with a bromine end group and capable of chain extension.

Finally, the degraded P(OEOMA300)-*block*-PS copolymers (copolymer 21H) formed a stable dispersion of relatively uniform spherical micelles consisting of a PS core and P(OEOMA300) corona, as shown in the TEM image (Figure S6). No aggregates were observed. The particle size was 226 ± 48 nm in diameter, as measured by TEM, compared with 445 nm (CV = 0.07) by DLS. These results confirm the successful chain extension of PS from the active Br functionality in the P(OEOMA300) nanogels. After degradation, P(OEOMA300)-*block*-PS copolymers were formed.

Conclusion

A new strategy was developed for the synthesis and functionalization of nanometer-sized colloidal particles of well-controlled, water-soluble polymers. This approach was accomplished by extending AGET ATRP to inverse miniemulsion. The successful synthesis of uncross-linked colloidal particles consisting of PEO-*block*-P(OEOMA) copolymers with $M_w/M_n < 1.3$ was demonstrated using OEOMA (OEOMA300 and OEOMA1100) macromonomers. The additional introduction of a disulfide-functionalized cross-linker into an inverse miniemulsion ATRP allowed for the synthesis of cross-linked nanogel particles. These particles showed excellent colloidal stability in dispersion media. DLS and AFM analysis indicated that the size was uniform for uncross-linked particles, and fairly

(59) Ali, M. M.; Stöever, H. D. H. *Macromolecules* **2004**, *37*, 5219−5227.
(60) Tsarevsky, N. V.; Min, K.; Jahed, N. M.; Gao, H.; Matyjaszewski, K. *ACS Symp. Ser.* **2006**, 939. In press.

uniform for cross-linked particles. The size determined by AFM analysis was 1.6−2.3 times larger, compared to the values determined by DLS measurements, due to flattening and adsorption of the particles on mica surface during the drying process.

The nanogels prepared by ATRP had several advantages over conventional RP-nanogels. When compared to RP-nanogels, the ATRP-nanogels had better colloidal stability in dispersion, and 1.6−1.8 times larger swelling ratios in different solvents including THF, toluene, and water. They degraded via reversible redox cleavage into individual polymeric chains with $M_w/M_n < 1.5$, indicating the formation of a uniform network, while the RP-nanogels failed to degrade. The uniform network can improve control over the release of encapsulated agents.

The successful chain extension of PS from ATRP-nanogels by ATRP was demonstrated by degradation experiments, HPLC chromatography, and micellization in water. These results indicated preservation of the bromine functionality on most of the polymeric chains in the ATRP-nanogels. The degraded P(OEOMA300)-*block*-PS copolymers self-assembled in water to stable, nanosized spherical micelles with PS core and P(OEOMA300) corona.

Acknowledgment. The support from NSF (DMR 05-49353) is gratefully acknowledged. We thank Ms. K. Min for synthesis of TPMA ligand, Mr. W. Tang for HPLC measurements of PEOMA526, Mr. J. Suhan for TEM measurements, and Dr. J. Spanswick and Mr. D. J. Siegwart for helpful discussions. J.K.O. thanks Natural Sciences and Engineering Research Council (NSERC) Canada for a postdoctoral fellowship.

Supporting Information Available: Experimental details including particle size distribution diagram, GPC diagram, and TEM image, and kinetic data for AGET ATRP of OEOMA1100, inverse miniemulsion RP, and chain extension of styrene from ATRP-nanogels. This material is available free of charge via the Internet at http://pubs.acs.org.

JA060586A